

# Fabrication of Cathode-supported Tubular Solid Oxide Electrolysis Cell for High Temperature Steam Electrolysis

Le Shao, Shaorong Wang\*, Jiqin Qian, Yanjie Xue and Renzhu Liu

CAS Key Laboratory of Materials for Energy Conversion, Shanghai Institute of Ceramics, Chinese Academy of Sciences, Shanghai 200050, China

Received: November 14, 2010, Accepted: February 14, 2011, Available online: April 29, 2011

**Abstract:** The cathode-supported tubular solid oxide electrolysis cell (SOEC) fabricated by dip-coating and co-sintering techniques have been studied for high temperature steam electrolysis application. The microstructure and electrochemical performances were investigated in both SOEC and solid oxide fuel cell (SOFC) modes. In SOFC model, the maximum power density reached 390.7, 311.0 and 248.3 mW cm<sup>-2</sup> at 850, 800, and 700 °C, respectively, running with H<sub>2</sub> (105 mL min<sup>-1</sup>) and O<sub>2</sub> (70 mL min<sup>-1</sup>) as working gases. In SOEC mode, the results indicated that the steam ratio had a strong impact on the performance of the tubular SOEC, and it's better to operate the tubular SOEC in high steam ratio. I-V curves and EIS results suggested that the microstructure of the tubular SOEC needs to be optimized for mass transportation.

**Keywords:** Solid oxide electrolysis, Hydrogen production, Tubular cell

## 1. INTRODUCTION

In recent years, hydrogen has been identified as a potential alternative fuel and an energy carrier for the future energy supply [1]. Fossil-fuel-free hydrogen production technologies are expected for future hydrogen energy society in order to avoid green-house gases emission. Water electrolysis is one of the important hydrogen production technologies which do not emit carbon dioxide [2]. In particular, high temperature steam electrolysis (HTSE) is a promising technology since it consumes less electrical energy as compared to low temperature water electrolysis, and a significant part of the energy demand for water electrolysis can be provided by heat-energy [3-5]. Theoretically, HTSE using solid oxide electrolysis cells (SOECs) can efficiently utilize renewable energy or advanced nuclear energy to produce hydrogen. It is also possible to operate the SOEC in reverse mode, as the solid oxide fuel cell (SOFC), to produce electricity [6-8]. Therefore, there has been remarkable works in this field [9-10].

Tubular SOFCs have many advantages such as ease in sealing and the ability to endure the thermal stress caused by rapid heating up to operating temperature [11-12], and have been widely investigated. However, there was little report on tubular solid oxide cells

used as SOEC for HTSE. In this study, the Ni-YSZ cathode-supported tubular SOECs were fabricated by dip-coating and co-sintering technology. Its microstructure and electrochemical properties were investigated and discussed.

## 2. EXPERIMENTAL

### 2.1. Fabrication of tubular SOECs

The cathode-supported thin tube consisted of a NiO-YSZ cathode, a NiO-Zr<sub>0.89</sub>Sc<sub>0.1</sub>Ce<sub>0.01</sub>O<sub>2-x</sub> (ScSZ, Scandia-stabilized zirconia, Daiichi Kigenso Kagaku Kogyo, Japan) (NiO-ScSZ) cathode functional layer, and a ScSZ electrolyte film, was fabricated using dip-coating and co-sintering techniques.

Before dip coating, the slurries of NiO-YSZ cathode, NiO-ScSZ cathode functional layer, and the ScSZ electrolyte were prepared by ball -milling method. For instance, the NiO-YSZ cathode slurry (50% NiO and 50% YSZ by mass) was first prepared. An azeotropic mixture of butanone and ethyl alcohol was used as solvent, triethanolamine as dispersant, polyethylene glycol as plasticizer, and poly-vinyl-butyl as the binder. All the organic additives were supplied by Shanghai Chem., China. The starting materials were weighed, mixed, ball-milled. The homogeneous slurry was then obtained. Other slurries were prepared in the same way but with different quantity of organic additives. The dip-coating proc-

\*To whom correspondence should be addressed: Email: srwang@mail.sic.ac.cn  
Phone/Fax.: 086-21-52411520

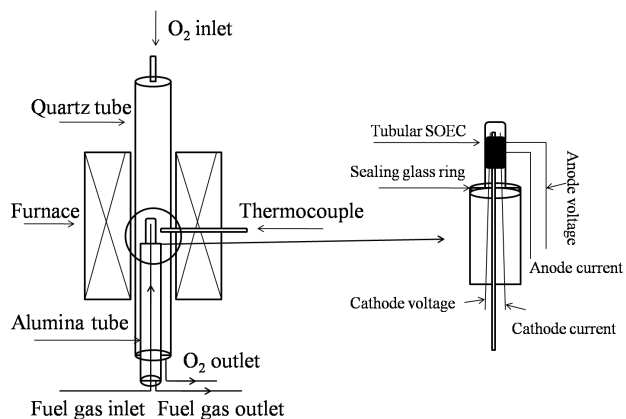


Figure 1. Schematic of the tubular SOEC test setup.

ess was carried out using a glass tube that was closed at one end. Firstly, the glass tube was dipped in the NiO-YSZ slurry for 15 s then slowly drawn up. This action was repeated five or six times to achieve the desired thickness. The tube was then dip-coated in NiO-ScSZ slurry for one time to prepare the NiO-ScSZ cathode functional layer. The tube dried at room temperature for 48 h, and then it was moved from the glass tube and cut to the required length and pre-sintered at 1000 °C for 2 h in air. The pre-sintering green tube was then dip-coated in ScSZ slurry to prepare electrolyte membrane. After drying, it was co-sintered at 1400 °C for 4 h in air. After all these process, the cathode supported electrolyte tube was obtained.

Secondly, the cathode supported electrolyte tube was dip-coated with LSF ( $\text{La}_{0.8}\text{Sr}_{0.2}\text{FeO}_3$ , synthesized by sol-gel self-propagating method)-ScSZ anode slurry. After drying, the tube was sintered at 1200 °C for 3 h in air to complete a cell. The fabricated tubular SOEC was 10 cm in length, 1.1 cm in outside diameter, and 10.0  $\text{cm}^2$  in anode area.

## 2.2. Characterization of tubular SOECs

The microstructure information was obtained from the scanning electron microscope (SEM, s-3400N, Hitachi, Japan) images of the cross section of the tubular SOEC after operation.

The tubular SOECs tests were carried out in the setup described in Fig.1. Steam was produced using a bubbler with precise temperature-control. The steam ratio in fuel gas ( $\text{H}_2$  and  $\text{N}_2$  mixture) was controlled by setting the bubbler temperature according to the standard saturation curve. Heater bands were installed between the bubbler and the water condenser for dew condensation prevention. During the test, pure hydrogen was flowed into the tubular SOEC for reducing NiO to Ni at 850 °C, firstly. Then the cells were tested in both SOEC and SOFC modes at different flow rates and steam ratios.  $I$ - $V$  curves were obtained by the volt-ampere method. The electrochemical impedance spectra (EIS) were obtained using an Electrochemical Workstation IM6ex (Zahner, GmbH, Germany). The measurements were performed in the frequency range of 0.03 Hz - 100 kHz with amplitude of 20 mV under open circuit state, or with electrolysis current density of 50  $\text{mA cm}^{-2}$ , respectively. The measurements were carried out at 750-850 °C, in steps of 50 °C.

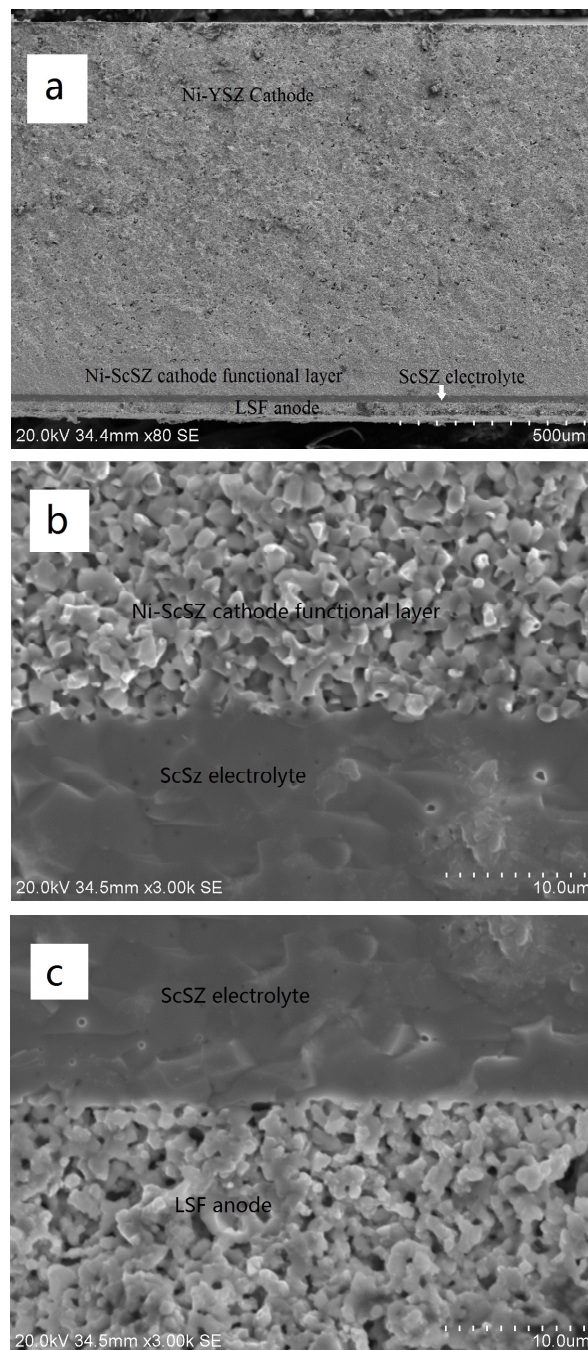


Figure 2. SEM images of the fabricated tubular SOEC after operation: (a) the whole cross section of the cell; (b) the interface between cathode and electrolyte; (c) the interface between electrolyte and anode.

## 3. RESULTS AND DISCUSSION

### 3.1. Microstructural characteristics of the tubular SOEC

Fig.2. shows SEM images of the tubular SOEC after operation. It can be seen from Fig.2 (a) that the tubular SOEC consisted of four

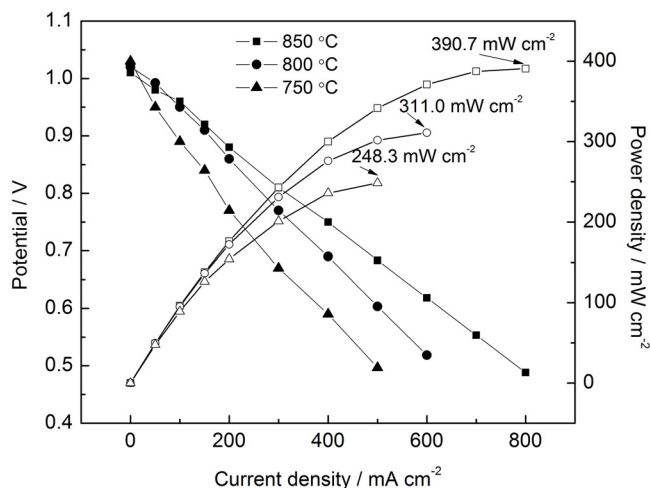


Figure 3. The  $I-V$ ,  $I-P$  curves of the tubular SOEC running with  $105 \text{ mL min}^{-1} \text{ H}_2$  and  $70 \text{ mL min}^{-1} \text{ O}_2$  in SOFC mode at three different temperatures.

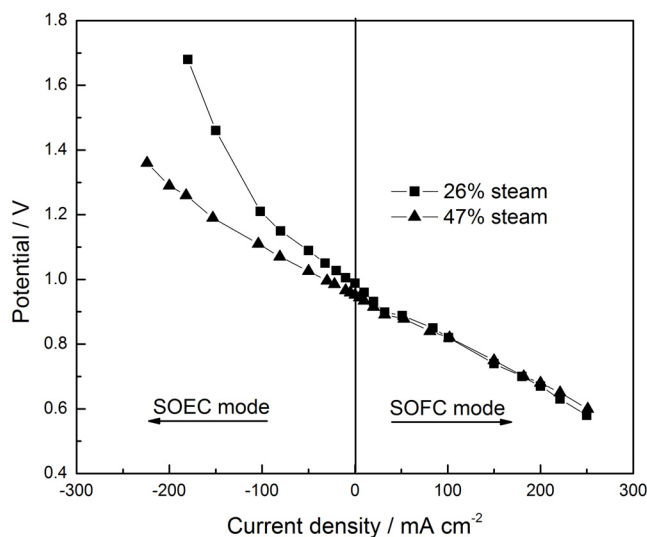


Figure 4. The  $I-V$  curves of the tubular SOEC operated with  $105 \text{ mL min}^{-1}$  fuel mixtures ( $\text{H}_2 / \text{N}_2 = 1 / 2$ ) of different steam ratios in both SOFC and SOEC modes at  $850 \text{ }^\circ\text{C}$ .

layers including Ni-YSZ cathode, Ni-ScSZ cathode functional layer, ScSZ electrolyte and LSF anode, and the thickness of each layer were 1200, 110, 27, and  $50 \text{ }\mu\text{m}$ , respectively. Fig.2 (b) shows that the interfaces between the Ni-ScSZ cathode functional layer and the ScSZ electrolyte integrated well, with no crack and exfoliation occurred, as shown in Fig. 2(c). The results suggested that the fabricated tubular SOECs could be operated in both SOEC and SOFC modes with no structure destruction.

### 3.2. Electrochemical performance of tubular SOEC

Fig.3. shows the typical  $I-V$ ,  $I-P$  curves of the tubular cell running with  $105 \text{ mL min}^{-1} \text{ H}_2$  and  $70 \text{ mL min}^{-1} \text{ O}_2$  in SOFC mode. It can be seen that the fabricated SOEC had good performances in

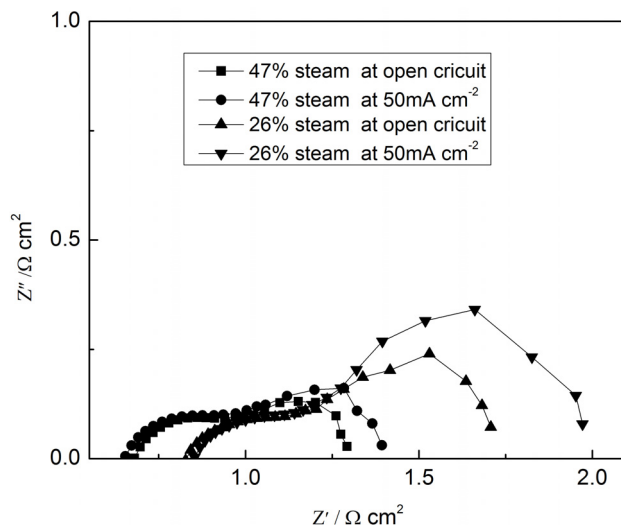


Figure 5. The EIS of the tubular SOEC operated with  $105 \text{ mL min}^{-1}$  fuel mixtures ( $\text{H}_2 / \text{N}_2 = 1 / 2$ ) of different steam ratios in open circuit state or a state of electrolysis current density of  $50 \text{ mA cm}^{-2}$  at  $850 \text{ }^\circ\text{C}$

SOFC mode, with maximum power densities of  $390.7$ ,  $311.0$ , and  $248.3 \text{ mW cm}^{-2}$  at  $850$ ,  $800$ , and  $700 \text{ }^\circ\text{C}$ , respectively, close to that of the tubular SOFC with a Sr-doped  $\text{LaMnO}_3$  cathode [13].

Fig.4. shows the typical  $I-V$  curves of the tubular SOECs operated at  $105 \text{ mL min}^{-1}$  of fuel mixtures ( $\text{H}_2/\text{N}_2=1/2$ ) combined with 47% and 26% steam in both SOFC and SOEC modes at  $850 \text{ }^\circ\text{C}$ . The open circuit voltage (OCV) for the SOECs at 47% and 26% steam were  $0.952$  and  $0.988$ , respectively, in agreement with the Nernst potential. It can be seen that the two  $I-V$  curves of the tubular cell running in SOFC mode show almost the same linearity and slope values at 47% and 26% steam. While in SOEC mode, the two curves show significant differences. For instance, the current densities of the cell in fuel with 26% and 47% steam, in SOFC mode, were  $200$  and  $197 \text{ mA cm}^{-2}$  under  $0.68 \text{ V}$ , whereas in SOEC mode, the values were  $135$  and  $224 \text{ mA cm}^{-2}$  under  $1.36 \text{ V}$ , respectively. This phenomena may be attributed to the cathode concentration polarization occurred at higher current densities [14]. The results indicated that the steam ratio had a strong impact on the performance of the tubular cell in SOEC mode, and it is better to operate the tubular SOEC at high steam ratio in order to avoid concentration polarization.

Fig.5. shows typical EIS of the tubular SOEC operated in the open circuit state or a state with electrolysis current density of  $50 \text{ mA cm}^{-2}$  in SOEC mode at  $850 \text{ }^\circ\text{C}$ . The total resistances in 47% and 26% steam were  $1.29$  and  $1.72 \text{ }\Omega \text{ cm}^2$  at open circuit, while the values at electrolysis current density of  $50 \text{ mA cm}^{-2}$  were  $1.39$  and  $1.98 \text{ }\Omega \text{ cm}^2$ , respectively. The total resistance increased when steam ratio decreased from 47% to 26%, indicating that the performance of the tubular decreased with the steam ratio, in agreement with the result obtained from Fig 4. The reason for the increase of bulk resistance (high frequency intercept) is not clear yet and needs to confirm in further work, the increase of polarization can be discussed here. It can be seen that each Nyquist plot consisted of a

small higher frequency depressed arc and a large lower frequency arc. With decreasing steam ratio, a pronounced increase in the lower frequency arc was observed, whereas the higher frequency arc changed slightly. It was known that the lower frequency arc was associated with gas diffusion [14, 15]. The increase in the lower frequency arc suggested that the gas diffusion becomes difficult when steam ration is decreased, so that the microstructure of the tubular SOEC should be optimized in the future for high temperature steam electrolysis.

#### 4. CONCLUSIONS

Tubular solid oxide cells were fabricated by dip-coating and co-sintering techniques. The obtained cells showed promising performances in SOFC mode. When they were operated in SOEC mode, however,  $I$ - $V$  curves and EIS results suggested that steam ratio had a strong impact on the performance of the tubular cell in SOEC mode. With the decrease of steam ratio, the concentration polarization occurred, so the tubular SOEC preferred to be operated at high steam ratio in order to avoid concentration polarization. These results showed that the microstructure of the tubular SOEC should be optimized further for high temperature steam electrolysis.

#### 5. ACKNOWLEDGEMENT

The authors are grateful for the financial support from the Science and Technology Commission of Shanghai Municipality No. 09DZ1206600.

#### REFERENCES

- [1] G. Marban, T. Valdes-Solis, *Int. J. Hydrogen Energy*, 32, 1625 (2007).
- [2] J.D. Holladay, J.Hu, D.L. King, Y. Wang, *Catalysis Today*, 139, 244 (2009).
- [3] A. Hauch, S.D. Ebbesen, M. Mogensen, *J. Mater. Chem.*, 18, 2331 (2008).
- [4] M. Ni, M. K. H. Leung, D.Y.C. Leung, *Int. J. Hydrogen Energy*, 33, 2337 (2008).
- [5] A. Briss, J. Schefold, M. Zahid, *Int. J. Hydrogen Energy*, 33, 5375 (2008).
- [6] V. Utgikar, T. Thiesen, *Int. J. Hydrogen Energy*, 31, 939 (2006).
- [7] Y. Shin, W. Park, J. Chang, J. Park, *Int. J. Hydrogen Energy*, 32, 1486 (2007).
- [8] S. Fujiwara, S. Kasai, H. Yamauchi, K. Yamada, S. Makino, K. Matsunaga, M. Yoshino, T. Kameda, T. Ogawa, S. Momma, E. Hoashi, *Progr. Nucl. Energy*, 50, 422 (2008).
- [9] C. Stoots, J. O'Brien, J. Hartvigsen, *Int. J. Hydrogen Energy*, 34, 4208 (2009).
- [10] J. Udagawa, P. Aguiar, N.P. Brandon, *J. Power Sources*, 180, 354 (2008).
- [11] N.M. Sammes, Y. Du, R. Bove, *J. Power Sources*, 145, 428 (2005).
- [12] K. Kendall, M. Palin, *J. Power Sources*, 71, 268 (1998).
- [13] R.Z. Liu, C. H. Zhao, J.L. Li, S.R. Wang, *J. Power Sources*, 195, 541 (2010).

- [14] Z.L. Zhan, W. Kobsiriphat, J.R. Wilson, *Energy & Fuels*, 23, 3089 (2009).
- [15] Z.L. Zhan, L. Zhao, *J. Solid State Electrochem*, 195, 7250 (2010).